Acta of Bioengineering and Biomechanics
Vol. 20, No. 1, 2018

Original paper
DOI://10.5277/ABB-01028-02

The comparative study of influence of lactic and glycolic acids copolymers type on properties of daunorubicin loaded nanoparticles and drug release

ELENA NIKOLSKAYA[1, 2]*, MARIYA SOKOL[1, 2], MARIYA FAUSTOVA[1, 2], OLGA ZHUNINA[2], MURAD MOLLAEV[1, 2], NIKITA YABBAROV[2], OKSANA TERESHCHENKO[2], ROMAN POPOV[1, 2], EUGEN SEVERIN[2]

[1] Moscow Technological University, Moscow, Russian Federation.
[2] Russian Research Center for Molecular Diagnostics and Therapy, Moscow, Russian Federation.

Purpose: The aim of this study was to compare the physico-chemical and biological properties of polymeric nanoparticles obtained from poly(DL-lactide-co-glycolide) (PLGA) with different ratios of monomers loaded with daunorubicin (DNR). *Methods:* DNR-loaded nanoparticles (NPs) were prepared with use of modified simultaneous double-emulsion solvent evaporation/diffusion technique. NPs were characterized using dynamic light scattering, atomic force microscopy, transmission electron microscopy, scanning electron microscopy, and differential scanning calorimetry and Fourier transform infrared spectroscopy. *Results:* NPs with DNR were differing in size and zeta potential, depending on the type of polymer. The data obtained show that total content of DNR correlates with the values of the binding constant of DNR with polymers. The release of DNR from NPs proceeds predominantly for polymers with lower binding constants. The *in vitro* study of NPs on the MCF-7 cells showed similar activity of particles and substances while for the anthracycline-resistant MCF-7Adr cells the cytotoxicity of the nanoparticles was 3 to 7 times higher depending on the type of copolymer. *Conclusions:* PLGA DNR-loaded nanoparticles can be used to overcome multidrug resistance (MDR) as well as for reducing the frequency of DNR reception due to the prolonged effect, which allows maintaining the concentration of the drug at the required level. The usefulness of binding constant calculations for obtaining nanoparticles with the maximum drug loading was proven. The rate of drug administration and the frequency of administration can be calculated based on the DNR release profiles and release parameters that depend on polymer type.

Key words: *nanoparticles, daunorubicin, PLGA, controlled release, MCF7/MCF7 Adr, dissociation constant*

1. Introduction

In recent years, significant effort has been devoted to development of optimal methods of drug delivery to target cells according to nanotechnology approach [5]. Nanotechnology focuses on formulating therapeutic agents in biocompatible nanocomposites, such as nanoparticles, nano-capsules or micellar systems [3]. Polymeric NPs have a polymeric shell and an inner core. The active drug is usually dissolved in the core, but may also be packed in the surface/subsurface region [13]. NPs have been extensively investigated in drug delivery systems for drug targeting because of their particle size ranging from 50 to 500 nm, which is acceptable for intravenous injection [16]. The proper drug delivery system should be not only biocompatible and biodegradable, but also poorly immunogenic, able to load the drug efficiently and do not change drug activity. This is extremely important for chemotherapeutic drugs. NPs with drugs are being increasingly used to improve drug efficacy, specificity, tolerability and therapeutic index [26]. During the last decade, a number of different polymers have been investigated for formulating biodegradable NPs [10], [19], with PLGA being the most popular [8]. PLGA

* Corresponding author: Elena Nikolskaya, Sympheropolsky Blvd, 8, 117638 Moscow, Russian Federation, Phone: +7(967)066-49-06, Fax: +7 (499) 613-23-5, E-mail: elenanikolskaja@gmail.com
Received: October 13th, 2017
Accepted for publication: December 21st, 2017

particles are not toxic and are eliminated from the body by the citric acid cycle as lactic and glycolic acids. The drug release from NPs depends on many factors: drug physicochemical properties (including solubility in water), drug-PLGA interactions, loading efficiency, diffusion of drug from the core to the surface, diffusion through the polymer, presence pores and channels concentration. The release of drugs in many cases is diffusion-controlled and described by various models based on Fick's law [1], [11]. The information obtained from release profiles enables prediction of NPs behavior *in vivo* as well as to calculate the rate of drug administration. The aim of this work was to compare of influence NPs formulation using different type of PLGA and examine the effect of DNR release from NPs, which depends mainly on the amount and type of polymer. Thus, the influence of pH values controlling release profiles was investigated as well as the mechanism of release and kinetics was determined using model-dependent method. As a model chemotherapy drug used to treat cancer DNR was tested. This choice was due to the fact that DNR is widely used for treatment of many tumor types in a free and in liposomal form, as well as the fact that the authors' team has extensive experience in the creation of the NPs with the anthracycline antibiotics [7], [15], [28]. The influence PLGA type on biological properties of DNR loaded nanoparticles was investigated *in vitro* on the MCF-7 and MCF-7 Adr cell lines.

2. Material and methods

2.1. Materials

In this work the following reagents were used: daunorubicin hydrochloride (Sigma-Aldrich, United States); Poly(DL-lactide-co-glycolide): PLGA-COOH 50/50 (PDLG 5002a), inherent viscosity: 0.2 dL/g in HFIP; PLGA-COOH 50/50 (PDLG 5004a), inherent viscosity: 0.4 dL/g in HFIP; PLGA 75/25 (PDLG 7507), inherent viscosity: 0.7 dL/g in HFIP; PLGA-COOH 75/25 (PDLG 7502a), inherent viscosity: 0.2 dL/g in HFIP; PLGA 75/25 (PDLG 7502), inherent viscosity: 0.2 dL/g in HFIP (PURASORB PURAC, The Nederlands); Poly(vinyl alcohol) (PVA), average Mw ~25,000, powder, 88% hydrolyzed (Sigma-Aldrich, United States); D-Mannitol (Sigma-Aldrich, United States); dichloromethane (DCM) and acetone (ACE) of chemical grade (Khimmed Syntes, Russia); gentamycin (ICN, United States); (3(4,5-dimethylthiazol-2-yl) -2,5-diphenyltetrazolium bromide (MTT, Sigma, United States); DMEM cell culture medium (Gibco, United States); 10% FBS (Gibco, United States); DMSO (ACS grade, Amresco, United States); Milli-Q (Millipore, Milli-Q Advantage A10, France); Tween 80 (Sigma-Aldrich, United States); trypsin (Sigma--Aldrich, United States); phosphate buffered saline (PBS, Amresco, United States); sodium hydrogencarbonate (Sigma-Aldrich, United States); ethylenediaminetetraacetic acid (EDTA, Sigma-Aldrich, United States); fetal bovine serum (FBS) (Hyclone, United States); Mowiol (CalBiochem, United States); tissue culture flasks (25 cm^2), 96-well plates (Corning--Costar, United States); Superose 6 (GE Healthcare Life Sciences, United States).

2.2. Preparation of NPs

DNR-loaded nanoparticles were prepared using modified simultaneous double-emulsion (water-in-oil--in-water) solvent evaporation/diffusion technique. Briefly, 100 mg of PLGA was dissolved in 5 ml organic mixture of DCM and ACE with ratios (4:1, v/v) containing Tween-80 (5%, v/v) as an emulsifier. DNR (10 mg) was dissolved in 0.5 ml of 2% $NaHCO_3$ and after 10 min of stirring 0.5 ml of distilled water was added, and then emulsified in the polymer solution through homogenization for 1 min × 3. The primary W/O emulsion was further added to 25 ml of aqueous solution of 0.5% PVA with US-homogenization (1 min × 3) to achieve the stable double emulsion (W/O/W). The residual organic solvents were evaporated under negative pressure and the nanoparticles suspended in emulsion were collected by liquid chromatography with Superose 6 column (50 × 5 cm), flow rate was 1 ml/min. Finally, the products with 100 mg of D-mannitol were dried by lyophilization and stored at 4 °C.

2.3. Characterization of NPs

2.3.1. Particle size, zeta-potential and PDI

The particle size was measured by the dynamic light scattering method and zeta potential, by electrophoresis. The sample was used for the preparation of 1 mg/ml suspension and the measurements were performed on a Zetasizer Nano ZS ZEN 3600 analyzer (Malvern Instruments, Great Britain) using a standardized protocol (SOP).

2.3.2. Entrapment Efficiency (EE %) and Drug Loading (DL %)

The DNR content of nanoparticles was analyzed by a spectrofluorometer (Hitachi 557). DNR-loaded nanoparticles (5 mg) were dissolved in dimethyl sulfoxide (DMSO, 1 ml). The fluorescence intensity of DNR in the solution was measured at 590 nm emission wavelength (with 470 nm excitation wavelength). The concentration of DNR was calculated from a standard curve prepared by measuring the fluorescence intensity of known concentrations of free DNR. Drug loading and encapsulation efficiency were calculated as follows:

Drug loading % *= (weight of remained drug in the nanoparticles / weight of polymeric nanoparticles) × 100*;

Encapsulation efficiency % *= ((total amount of drug – actual amount of drug in supernatant) / total amount of drug)) × 100.*

2.4. Surface morphology of PLGA nanoparticles

2.4.1. Transmission electron microscopy (TEM) and scanning electron microscopy (SEM)

Shape and surface morphology of nanoparticles were examined with TEM (Osiris FEI, USA) and SEM (JEOL, JSM-7401F, Japan). For TEM a drop of particle suspension with concentration 1 mg/ml was placed on a 3 mm copper grid covered with Formvar film and dried for 30 min. For SEM the lyophilized nanoparticles were placed on a double stick tape over aluminum stubs to get a uniform layer of particles. Then, the air-dried sample was scanned at 0.5 kV.

2.4.2. Atomic force microscopy (AFM)

In a relevant atomic force microscopy study (AFM), 5 μl of nanoparticle suspension (1 mg/ml) was deposited onto freshly cleaved mica (already glued on a steel disk) and water was allowed to evaporate for 30 min at room temperature. Images were taken by AFM (NT-MDT NEXT, Russia) in tapping mode and operating in air at room temperature.

2.5. Determining of dissociation constant of the PLGA-DNR complex

The polymers were dissolved in 3 ml of ACE to achieve mass concentrations of 1, 2, 3, 4, 5, 6, 7, 8, 9 and 10%. Afterwards, 30 μg of daunorubicin dissolved in 30 μl of water were added dropwise. The interval between receiving and measuring the resulting PLGA-DNR complexes was 10 min. The optical density of the complex was measured with a Thermo Spectronic Helιosα spectrophotometer in the 200–600 nm range against a mixture of solvents (30 μl of water in 3 ml of ACE). Calculations were carried out for values at a wavelength of 481 nm.

2.6. FTIR analysis

To perform a Fourier transform infrared spectroscopy (FTIR) analysis, the samples were prepared using a KBr (infrared grade) powder technique. The samples were studied using FTIR EQUINOX 55 in the wavenumber range from 400 to 4,000 cm^{-1}.

2.7. Thermal analysis

The physical state of DNR inside the nanoparticles was investigated by differential scanning calorimetry (DSC) DSC 204 F1 Phoenix NETZSCH (Germany). Samples were cooled from room temperature (25 °C) to 15 °C at a rate of 5 K/min. Then samples were heated to 250 °C at a rate of 5 K/min. To accurately determine the heat and melting of the material, the DSC curve was measured twice. To prevent oxidation of the samples, heating was carried out in an argon atmosphere.

2.8. *In vitro* release profiles

The rate of the DNR release from the nanoparticles was evaluated in the phosphate-buffered saline (PBS) solution. Briefly, 50 mg of lyophilized DNR-loaded nanoparticles were suspended in 30 ml of 1 M PBS (pH 7.4 and 5.0). The samples were termostated at 37 °C with continuous agitation at about 100 rpm. At various preset intervals, the supernatant was withdrawn after centrifugation at 16000 rpm for 30 min. The supernatant was lyophilized and dissolved in 1 mL DMSO and the amount of DNR released was measured by the spectrophotometer (λ = 481 nm). Each drug release experiment was repeated three times.

2.9. Tumor cells

The human breast adenocarcinoma cell lines MCF-7 and MCF-7Adr were cultured in DMEM supple-

mented with 10% FBS at 37 °C in a humidified atmosphere containing 5% CO_2.

2.10. Cytotoxicity assays

Cytotoxicity of free DNR, DNR-loaded nanoparticles and empty nanoparticles was determined by measuring the inhibition of the cell growth using a tetrazolium dye (MTT) assay [16]. MCF-7, MCF-7 Adr cells were seeded on a 96-well plate. Following the cells were incubated for 72 h with various concentrations (0.78–25 μM) of free DNR, DNR-loaded nanoparticles and empty nanoparticles. Then cell viability was determined using MTT assay. Absorbance was measured using a microplate reader (Labsystems, Finland) at 540 nm. The MTT absorbance depends on the quantity of metabolically active cells. The IC50 value (drug concentration resulting in the 50% inhibition of growth, compared to reference) was directly determined from the dose-response.

2.11. Statistical analysis

OriginPro 8 SRO (OriginLab Corporation, United States), Excel (Microsoft), and Statistica 8 (StatSoft) programs were used for plotting and statistical analysis.

3. Results

3.1. Preparation of NPs and characterization

After selecting the optimal parameters of the technological process for obtaining polymeric nanoparticles, we investigated the effect of the type of polymer on the physico-chemical characteristics of the particles produced. For this experiment, copolymers of lactic and glycolic acids with different ratios of monomer and

Table 1. The effect of the lactic glycolic acid ratio on the size, PDI, zeta potential and encapsulation efficiency PLGA nanoparticles

Sample	EE, %	DL, %	Size, nm	Zeta potential, mV	PDI	Polymer type	Inherent viscosity, dL/g
DNR-NP1	73.35	2.22	161.2 ± 1.4	–23.5 ± 3.9	0.178	PDLG5002a	0.2
NP1	–	–	207.3 ± 1.3	–20.6 ± 4.1	0.220	PDLG5002a	0.2
DNR-NP2	72.72	2.20	184.4 ± 0.5	–10.4 ± 3.4	0.059	PDLG5004a	0.4
NP2	–	–	194.1 ± 2.9	–17.9 ± 1.9	0.141	PDLG5004a	0.4
DNR-NP3	55.57	1.31	184.3 ± 1.3	–25.3 ± 4.2	0.139	PDLG7502a	0.2
NP3	–	–	278.7 ± 3.8	–22.3 ± 2.6	0.210	PDLG7502a	0.2
DNR-NP4	57.85	1.82	176.1 ± 1.0	–9.1 ± 2.8	0.072	PDLG7502	0.2
NP4	–	–	251.0 ± 1.7	–18.0 ± 2.1	0.157	PDLG7502	0.2
DNR-NP5	53.23	1.05	219.8 ± 0.4	–6.2 ± 0.8	0.114	PDLG7507	0.7
NP5	–	–	243.3 ± 1.8	–23.1 ± 5.1	0.164	PDLG7507	0.7

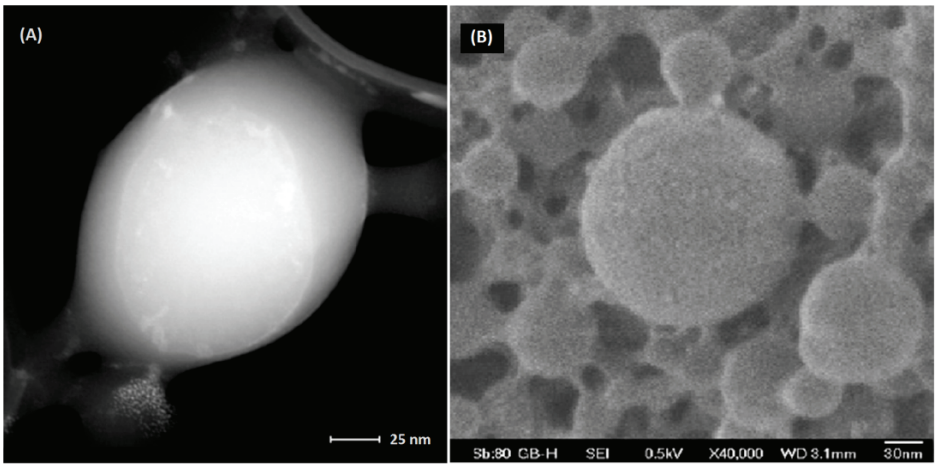

Fig. 1. TEM (A) and SEM (B) photomicrographs of DNR-NP1. Bars represent: 25 nm on (A) and 30 nm on (B)

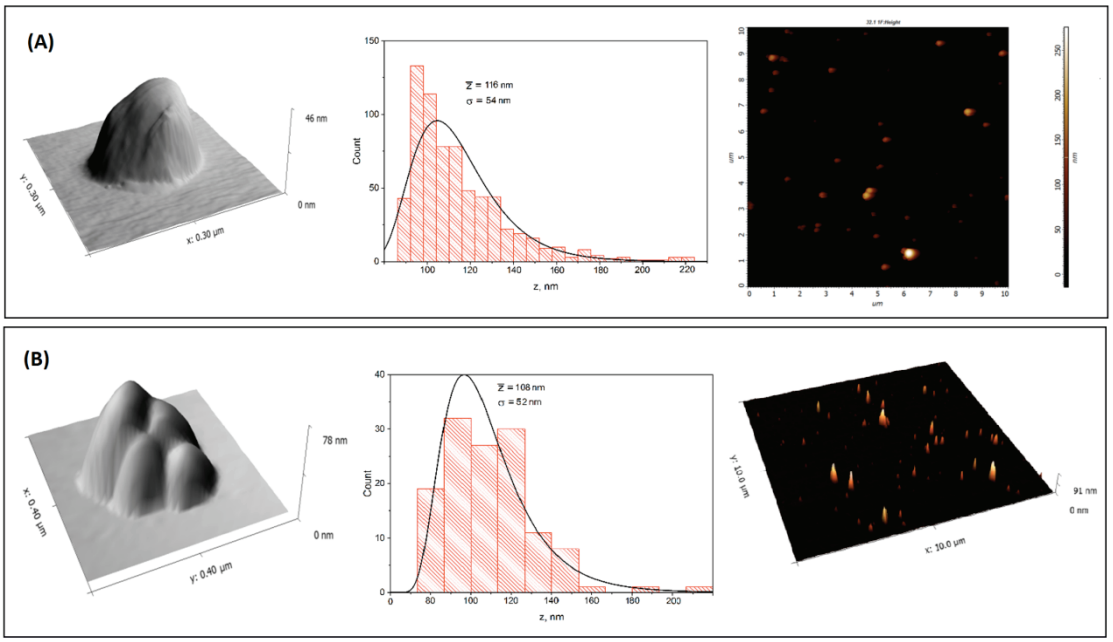

Fig. 2. Histogram of height measurements by AFM of the DNR-NP1 (A) and NP1 (B) spherical nanoparticles population with the log-normal distribution fit from the mean value and the standard deviation

viscosity were used (Table 1). For each batch of particles containing DNR, empty particles (without DNR, but produced in the similar way) were obtained as a negative control in further experiments. Main characteristics of the obtained particles are shown in Table 1.

The morphology of NPs was examined with the use of scanning electron microscopy (SEM), transmission electron microscopy (TEM) (Fig. 1) and atomic force microscopy (AFM) (Fig. 2). Only DNR-NP1 and NP1 results are shown in the paper, but the same techniques were used for all NPs. As can be seen from Fig. 1, prepared nanoparticles were spherical in shape.

In our study, AFM images of DNR-NP1 and NP1 nanoparticles have been studied in order to obtain a sufficient number of single NPs. The size distribution is shown in Fig. 2. The mean diameter value obtained from counting 687 NPs of DNR-NP1 type was 116 nm (standard deviation of 54 nm) while that of counting 130 NPs of NP1 type was 108 nm (standard deviation of 52 nm).

3.2. Calculation of dissociation constant of the PLGA-DNR complex

Calculation was performed to determine the dissociation constant of the PLGA-DNR complexes. To accomplish the task, we calculated the polymer weighed masses with the formula 1 to achieve mass concentrations of 1, 2, 3, 4, 5, 6, 7, 8, 9 and 10%. To the polymer solution 30 µg of DNR dissolved in 30 µl of water were added.

It is also worth noting that the values of the optical densities for solutions with a mass concentration of 9 and 10% were almost the same, therefore, it can be concluded that maximal binding of DNR with polymers was reached. The concentration that can be observed at a wavelength of 481 nm corresponds to the value of free drug, which is not bound to the complex with the polymer. By formula 1 were recalculated mass batches of PLGA relevant mass concentrations given mass of daunorubicin dissolved in water [14]. W was in the range of 1–10 (mass %).

$$W = m(\text{PLGA})/[m(\text{PLGA}) + m(\text{H}_2\text{O}) + m(\text{DNR})] \quad (1)$$

The molar concentration of DNR [DNR] was calculated from formula (2):

$$[\text{DNR}] = V_{\text{H2O}} * \rho/Mw * V = 1.896 * 10^{-5}\ \text{Mol/L} \quad (2)$$

where $V = 3.030$ ml.

The molar concentration of the polymer [P] was calculated with the formula (3):

$$[\text{P}] = [(m(\text{PLGA}) / Mw)]/V \quad (3)$$

where $V = 3.030$ ml, [P], Mol/L.

According to molar concentrations of polymer and DNR, the following values were calculated: $Y = A/([\text{P}] * [\text{DNR}])$ – the ratio of the product of the optical density and the sum of the equilibrium concentrations of the polymer and DNR to the product of the

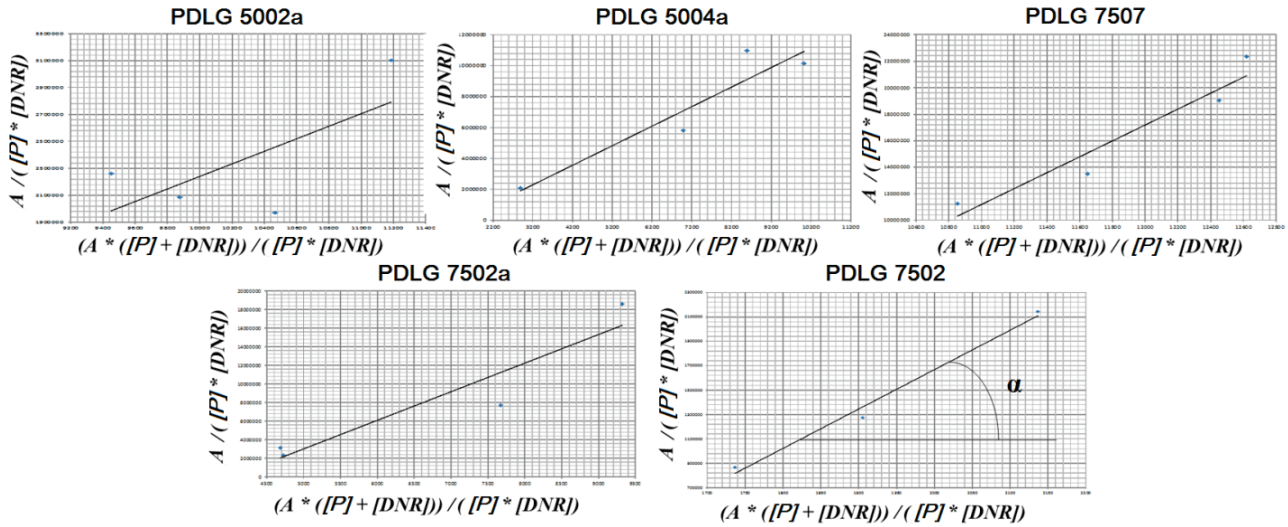

Fig. 3. Graphs with trend lines plotted in coordinates $Y = A/([P] * [DNR])$ and $X = (A * ([P] + [DNR])) / ([P] * [DNR])$

Table 2. Comparison of dissociation constant of the PLGA-DNR complex, DL and EE (%) of DNR-loaded nanoparticles, depending on the polymer type

PLGA	PDLG5002a	PDLG5004a	PDLG7507	PDLG7502a	PDLG7502
K_a	199560	1167	6250	3077	3333
$K_d = 1/K_a$	$5.01 * 10^{-6}$	$8.6 * 10^{-4}$	$1.6 * 10^{-4}$	$3.25 * 10^{-4}$	$3 * 10^{-4}$
DL, %	2.22	2.20	1.05	1.31	1.82
EE, %	73.35	72.72	53.23	55.57	57.85

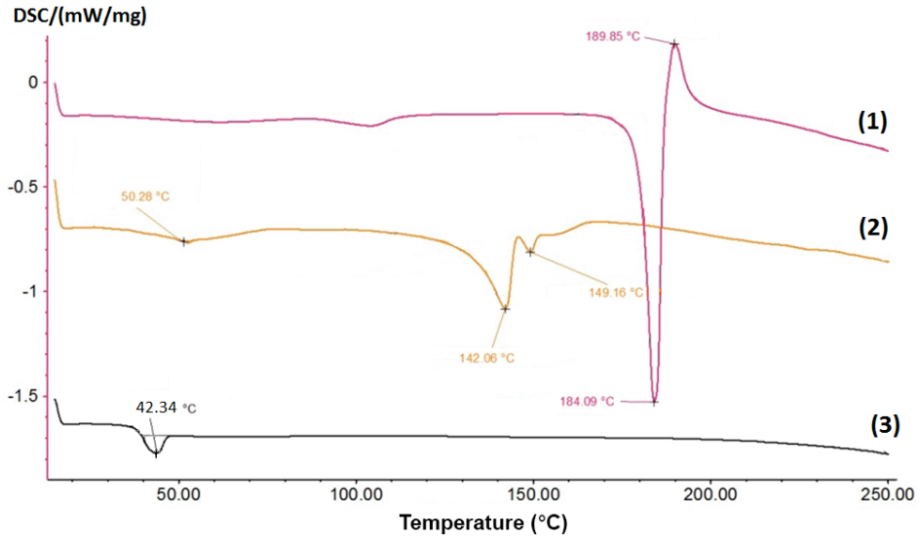

Fig.4. Differential scanning calorimetry (DSC) thermograms of free DNR (1), DNR-loaded nanoparticles (2) and PLGA (3)

same equilibrium concentrations; and $X = (A * ([P] + [DNR])) /([P] * [DNR])$ – the optical density of the complex to the equilibrium concentrations of the complex components. In the obtained coordinates, graphs were constructed and trend lines were drawn (Fig. 3) [2].

According to the graphs, the binding and dissociation constants were calculated using formula (4):

$$K_a = k_a/k_d = \mathrm{tg}\alpha = 1/K_d \quad (4)$$

The results of calculations showed that DNR complexes with PGLG5002a, PGLG5004a have the highest binding constant (Table 2).

DNR has the greatest affinity for the polymer PDLG5002a, so the nanoparticles obtained from this polymer were investigated by DSC and FTIR methods (Figs. 4 and 5).

3.3. Thermal analysis

Samples were attained from free DNR (1), DNR-loaded NPs (2) and PLGA (3). The samples were heated from room temperature up to 250 °C under nitrogen flow at a rate of 10 °C/min to determine the temperature range for structural transformations. As can be seen in Fig. 4, the glass transition temperature (*Tg*) was around 42–50 °C on both DSC curves for PLGA and DNR-loaded NPs, which was also in agreement with the observed *Tg* of PLGA, reported in the literature (between 40 and 60 °C) [6]. DNR had a melting point around 184 °C presented as an endothermic peak attributed to crystallization.

3.4. FTIR analysis

To confirm the stability of the substances in polymer forms and to determine the presence of interaction between the substances encapsulated in the polymer matrix and the polymer, FTIR spectroscopy was applied (Fig. 5).

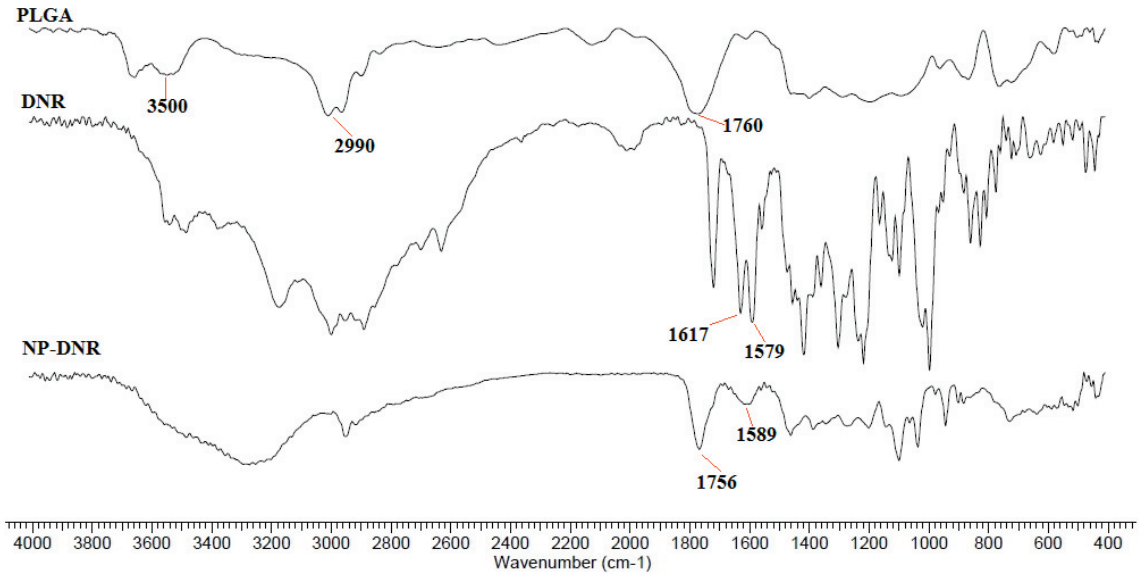

Fig. 5. FTIR spectrum of PLGA, free DNR and DNR-loaded PLGA nanoparticles (NP-DNR)

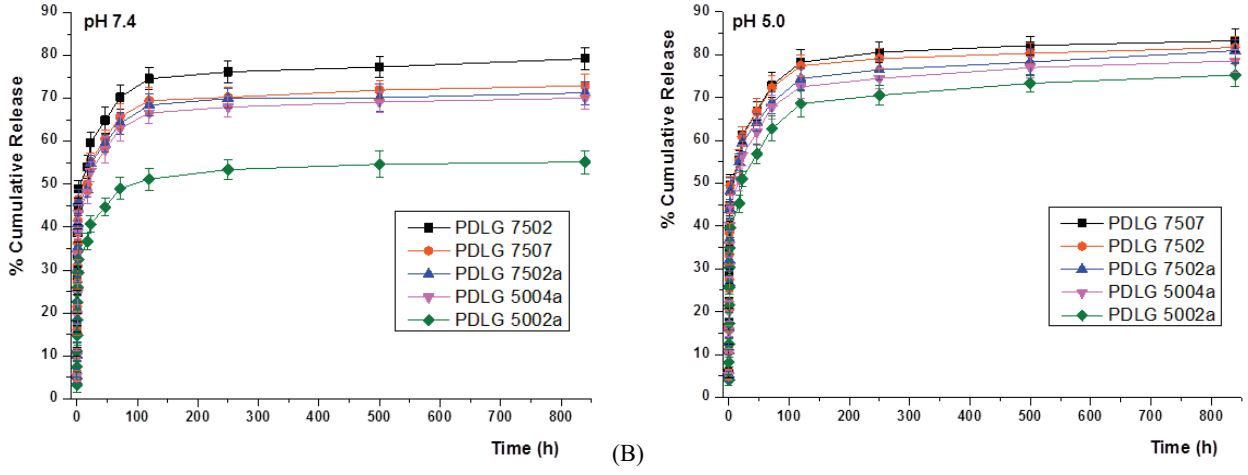

Fig. 6. *In vitro* release profile of daunorubicin at 37 ± 0.5 °C from polymeric nanoparticles at different pH values: (A) pH 7.4, (B) pH 5.0. Bars represent mean ± SD ($n = 3$)

3.5. Drug release kinetics

The DNR-loaded nanoparticles shows biphasic drug release pattern (Fig. 6). The initial burst release of free substance about 50% during the first 2.5 h was observed for polymers PDLG7507, PDLG7502 and PDLG7502a and about 40% and 50% for 20 h for polymers PDLG5004a and PDLG5002a, respectively. This burst phase is followed by a phase of relatively slow release of the substance, as previously reported [20], [24].

To determine the mechanism of release and its kinetics a model-dependent method was applied. According to the initial amount of substance during the burst released F_0 zero-order, first-order, Hixson–Crowell (H-C), Higuchi, Korsemeyer–Peppas (K–P) and a modified K–P model, were chosen for the mathematical description of the daunorubicin release kinetics for each type of polymer. The processing of statistical data and the selection of the release mathematical model was performed by an add-in DDsolver® [13]. To determine the accuracy of the approximation, the correlation coefficient R^2 was used. The method based on the calculation of R^2 is widely used and suitable for cases with the similar model equations parameters [1].

Based on the results of calculations (data not shown), the best approximation was achieved with K–P models and the parameter F_0 (R^2 values from 0.9213 till 0.9381). The mathematical model calculation was performed using formula 5.

$$M_t/M_\infty = kt^n \tag{5}$$

where M_t/M_∞ – the amount of the drug released at the time t, k – release rate constant and n (release exponent) – parameter indicating the mechanism of substance transfer.

For each type of polymer, the exponent and the release constant were calculated. The obtained data is presented in Table 3.

Similarity of release dissolution profiles at pH 7.4 and pH 5.0 was estimated by calculating the similarity factor (f_2) (Table 4). f_2 is a logarithmic transformation of the average of the squared vertical distances between mean dissolution values of two batches at each dissolution time point as shown in formula 6:

$$f_2 = 50 * \mathrm{Log}\{[1 + (1/n) * \sum_{t=1}^{n} (R_t - T_t)^2]^{-0.5} * 100\} \tag{6}$$

where Log – logarithm of a base 10, n – number of sampling time points, $\sum$ – summation over all time points, R_t and T_t are reference and test dissolution values (mean of at least 12 dosage units) at time point t.

The maximum distance between mean dissolution profiles at any time point cannot exceed 100%, in which case the value of f_2 will be close to zero. An average difference of 10% at all measured time points results in a f_2 value of 50 [4]. Therefore, it is believed that values of f_2 greater than 50 (50–100) indicate the equivalence of two profiles [18].

Table 3. Values of the K–P model parameters for the release of daunorubicin from the polymeric nanoparticles

NPs	pH	k	n
DNR-NP1	pH 7.4	25.755	0.128
	pH 5	30.457	0.149
DNR-NP2	pH 7.4	33.978	0.123
	pH 5	35.269	0.133
DNR-NP3	pH 7.4	35.624	0.119
	pH 5	37.539	0.128
DNR-NP4	pH 7.4	38.476	0.122
	pH 5	38.733	0.126
DNR-NP5	pH 7.4	36.276	0.119
	pH 5	38.952	0.128

3.6. *In vitro* toxicity

The results of DNR-loaded NPs on MCF-7 and MCF-7 Adr were performed (Fig. 7). As a negative control, empty NPs were used at identical concentrations corresponding to each batch of particles.

The IC50 values for DNR and DNR-loaded nanoparticles are presented in Table 5. The cytotoxic activity of NPs on the MCF-7 cell line was similar to that of free DNR, while an increase of NPs activity from 3 to 7 times on the MCF-7 Adr cell line was observed.

Table 4. Values of f_2 for dissolution profiles of DNR-loaded NPs at different pH (7.4 and 5.0)

	DNR-NP1	DNR-NP2	DNR-NP3	DNR-NP4	DNR-NP5
f_2 pH 7.4 and 5.0	57.3	79.64	74.1	93.3	69.7

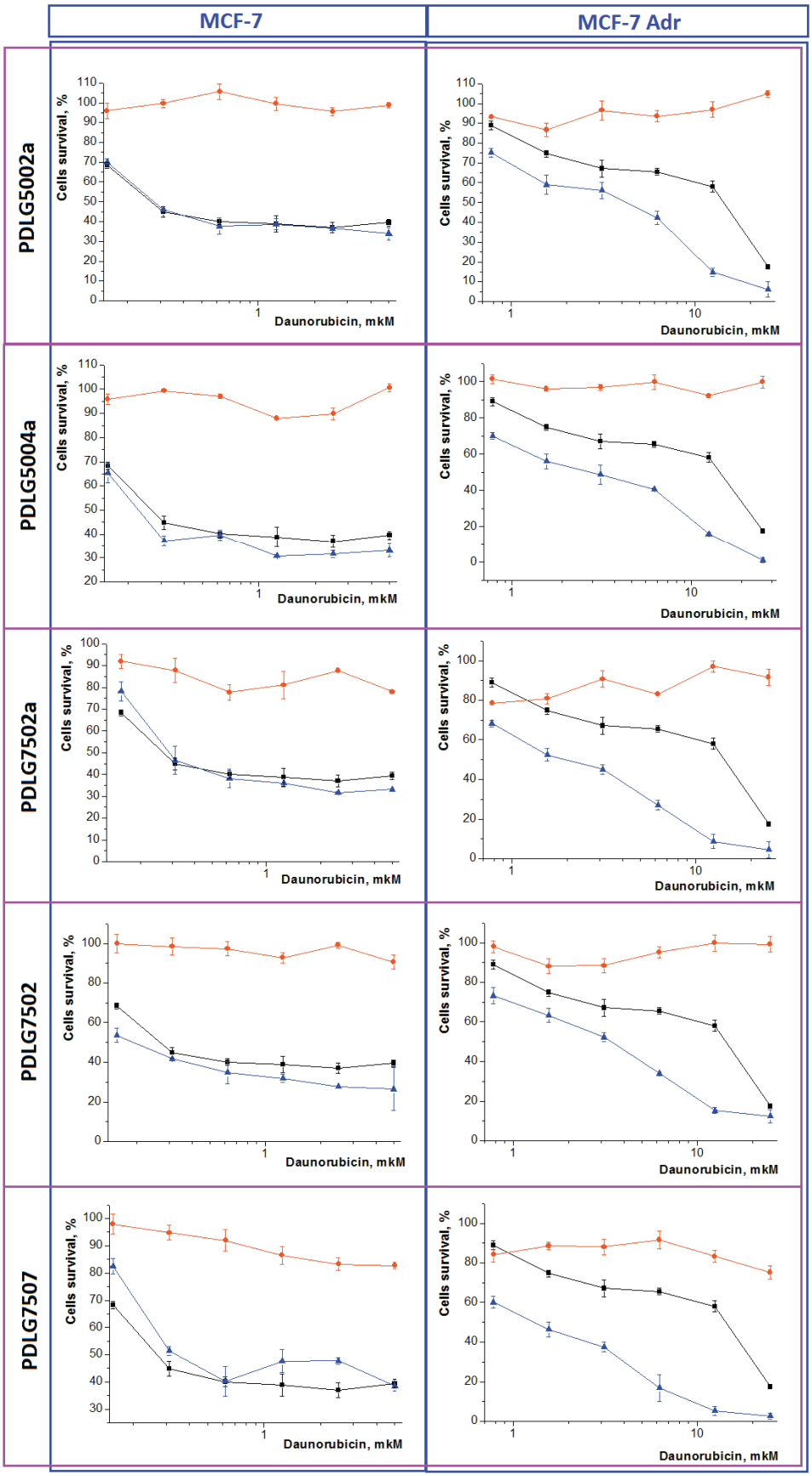

Fig. 7. Cells viability of free DNR (black line), different type of PLGA DNR-loaded nanoparticles (blue line) and empty PLGA nanoparticles (red line) after 72 h on MCF-7 (left) cells and MCF-7 Adr (right) cells (data are presented as the mean ± SD, $n = 3$)

Table 5. Values of IC50 for DNR and DNR-loaded nanoparticles on MCF-7 and MCF-7 Adr cell lines

IC50, μM	DNR	DNR-NP1 (PDLG5002a)	DNR-NP2 (PDLG5004a)	DNR-NP3 (PDLG7502a)	DNR-NP4 (PDLG7502)	DNR-NP5 (PDLG7507)
MCF-7	0.268	0.279	0.228	0.287	0.187	0.336
MCF-7 Adr	14.49	4.31	2.80	1.927	3.44	1.87

4. Discussion

4.1. Preparation of NPs and characterization

In previous research we developed a method for obtaining DNR-loaded PLGA nanoparticles [7]. Nanoparticles were prepared by the modified W/O/W double emulsion-solvent evaporation/diffusion method with preliminary transfer of daunorubicin into the base form by addition of $NaHCO_3$ to neutralize hydrochloride form of DNR. It was proven that the physical and chemical properties of the copolymer affect the final properties of the particles.

The results contained in Table 1 showed that the physical and chemical properties of the copolymer affect the final properties of the particles. Thus, when polymers with a viscosity of 0.2 dl/g and 0.4 dl/g are used, smaller particles can be obtained, so an increase of viscosity to 0.7 dl/g leads to increasing particle size (DNR-NP5 and NP5). The ratio of the monomer units also affects the properties. With an increase in the amount of lactic acid (75/25), both the average particle size and the range of their distribution increase. In polymers with the amount of lactic acid 75/25 (DNR--NP3, DNR-NP4, DNR-NP5) a decrease in the drug loading along with an increase in the inherent viscosity (DNR-NP5) was observed. The values of the zeta potential also depend on the type of copolymer. It can be noted that viscous or containing predominantly lactic acid polymers cause decrease in negative charge, especially for DNR containing particles (Table 1).

During production of empty particles, formation of agglomerates in all batches was observed leading to an increase in PDI values. It can be explained by formation of the polymer-substance complex (PLGA-DNR complex) while producing the NPs. The PLGA-DNR complex has amphiphilic properties due to the hydrophobic part of PLGA and hydrophilic part of DNR. These amphiphilic properties can be compared with those of PLGA-PEG copolymers from which small size nanoparticles can be obtained. In the case of empty nanoparticles (NP1-NP5) made of only hydrophobic PLGA, NPs formed an have increased size and PDI.

It was shown that the size values obtained with TEM and AFM are smaller than the hydrodynamic diameter determined by the DLS method. A similar effect has already been described earlier for PLGA--based nanoparticles [9]. Probably, the difference in these parameters arises as a result of the bulk hydrate shell covering the surface of nanoparticles. This hydrated shell is caused by the presence of a hydrophilic PVA associated with the surface of the nanoparticles.

Also, the difference in size may be caused by drying out of the nanoparticles during the preparation of a sample for microscopic examination. At the same time, the particles lose hydrate shell, which is present in the solution. To assess the biological activity, apparently, it is necessary to take into account the hydrodynamic diameter of the particles. It should be noticed, that the size values obtained with TEM, SEM and AFM correlate with each other.

4.2. Calculation of dissociation constant of the PLGA-DNR complex

An increase in the degree of DNR incorporation with the use of copolymers with a carboxyl group at the end was demonstrated (Table 1), this finding can be explained by sorption and formation of the polymer-substance complex. The values indicated in Table 2 show that polymer PDLG5002a has the best binding to DNR – this is confirmed by its lowest value of the dissociation constant among other polymers, and also by the highest content of DNR in the nanoparticles obtained (DNR-NP1). It should be noted that the terminal carboxyl group of the polymer in this case do not affect the degree of binding in the PLGA-DNR complex, while the ratio of lactic and glycolic acids has a significant effect (polymers 50/50 have the best affinity) and polymer viscosity (polymers with viscosity of 0.2 dl/g have the lowest constants among their groups). Thus, this method proved its efficacy to determine the equilibrium constants for the prediction of properties of polymeric nanoparticles composition with the highest content of the drug.

4.3. Thermal analysis

DSC was used to investigate the thermal transformations in NPs and provide insight into the state of a drug in NPs. The absence of a melting point peak for DNR-loaded NPs at 184 °C may be the result of the encapsulation process. Thus, we can suggest that DNR in NPs converted to the amorphous phase from the crystalline phase, in other words, the encapsulation process, disrupted formation of DNR crystals, which ensured the drug stability in NPs. The endothermic minor peaks at 142 °C and 149 °C likely were due to the presence of surfactant (PVA) in small amount in the formulation [27].

4.4. FTIR analysis

The FTIR spectrum of DNR-loaded nanoparticles (Fig. 5) shows the two characteristic bands assigned to the stretching of the carbonyl groups at 1617 cm^{-1} (less intense) and to the aromatic ring (C=C) stretching at 1579 cm^{-1} of DNR molecule is not observed in NP-DNR. There are all the characteristic peaks of the PLGA (3500, 2990, 1760 cm^{-1}), but with a slight shift, which indicates formation of new bonds with DNR. The band at 1756 cm^{-1} assigned to the carbonyl groups appears with reduced intensity. These findings are the evidence of the presence of drug molecules within the PLGA nanoparticles [12]. Absence of characteristic bands assigned to the stretching of DNR molecule on NP-DNR may indicate participation these groups in the formation of a new bonds.

4.5. Drug release kinetics

The type of polymer as well as formation of polymer-drug complexes can affect the profile of the DNR release kinetics from polymeric nanoparticles. The pH value strongly affects the kinetics of drug release. Thus, at more acidic pH values (5.0), the release proceeds at a higher rate and is most complete for all types of polymers. At the same time, at neutral pH values, the percentage of free DNR at the end of the experiment (800 h) is less, especially for polymer PDLG5002a. The results are correlated with DL and EE as well as with calculations of the dissociation constant (Table 2), thereby, they confirm the effectiveness of our method for selecting the optimal polymer for obtaining nanoparticles with maximum sorption of the drug. Also, based on the dissociation constant, the release rate of the drug can be assumed from the NPs.

The DNR-loaded NPs show biphasic drug release pattern with initial burst release and the next phase of slow release, which is typical for the diffusion of substance from the internal cavities of the particles and the onset of hydrolytic processes leading to degradation of the polymer [10]. The initial burst release of the drug can be associated with the dissolution and release of a drug absorbed on the polymer surface and with the diffusion of a substance near the surface of the NPs [22], [23].

To determine the mechanism of release and its kinetics a model-dependent method was applied. The mechanism of the first 60% drug release from NPs was determined by the K-P model. This model can be used to analyze release data of water-soluble substances from the polymers [21]. All parameters of K-P model (n and k) were calculated.

Interpretation of the values of n was carried according to the assumptions of Peppas: $n = 0.5$ (0.45) for the Fick diffusion mechanism; $0.5 < n < 1$ (0.89) for anomalous diffusion; $n > 1$ super case 2 transport (relaxation) [25], [26]. In the K-P model for spherical particles, the value of n equal to 0.45 indicates the Fick diffusion. However, for polydisperse systems, values below are possible [24]. Based on the calculated values of n, it was assumed that the diffusion of the substance proceeds according to Fick's law. The values of k for particles DNR-NP1 differ from the others. The release from these particles proceeded slower, which correlates with the data obtained in the study of the binding constant (Table 2). The similarity factor (f_2) was calculated and it was concluded that the DNR release profiles are similar at different pH values for all types of polymers.

4.6. *In vitro* toxicity

To confirm the cytotoxic properties of the obtained polymeric DNR-loaded nanoparticles, experiments on tumor cells of the human breast adenocarcinoma MCF-7 and the line resistant to the action of anthracycline antibiotics, in particular to doxorubicin, MCF-7 Adr were performed. According to the *in vitro* study (Fig. 7), it can be concluded that the PLGA DNR-loaded nanoparticles on the MCF-7 cell line, are comparably effective to the free DNR. This indicates that the biological activity of the DNR did not change after incorporation into the polymeric matrix.

Concerning the same resistant line of MCF-7 Adr cells, a significant increase in the cytotoxic activity of

all polymeric DNR-loaded NPs from 3 to 7 times can be noted, and it indicates a partial overcoming of MDR. Higher cytotoxicity of NPs on the MCF-7 Adr cell line than that of free DNR can be presumably explained by ABC-transporters activity. In the case of free DNR, molecules permeated into cells are subjected to efflux quite rapidly due to Pgp-protein activity. In the case of NPs, after its addition into cell culture DNR release is initiated immediately. Released DNR cannot reveal activity due to the resistant phenotype on the MCF-7 Adr cells, but DNR-loaded NPs internalization process continues, part of the DNR released into endo-lysosomal compartments being migrated into the nucleus and develops a cytotoxic effect.

It can be noticed that NPs prepared from different types of PLGA do not significantly differ in their cytotoxic activities. Also, it is observed the similarity in curves profiles all NPs is observed, which can explain identical properties and intracellular penetration mechanism.

5. Conclusions

Nanoparticles from various types of PLGA were prepared with the use of the modified W/O/W double emulsion-solvent evaporation/diffusion method. The physico-chemical parameters of the obtained nanoparticles demonstrate the effect of the type of polymer on the size, zeta potential and the degree of DNR incorporation. The best results were obtained when the polymer PDLG5002a was used. Calculations of the dissociation constant also showed the effect of the polymer type and its viscosity on the degree of drug affinity to the polymer. This method is useful for optimal polymer selection for obtaining NPs with the maximum drug loading. In the DNR release study the identity of the release profiles at different pH values was proved, and mathematical modeling was performed. In the study of cytotoxicity, the effectiveness of NPs on the MCF-7 cell line and the partial overcoming of MDR in the resistant line MCF-7 Adr have been proven. It can be noticed that NPs prepared from different types of PLGA do not significantly differ in their cytotoxic activities. Also, similarity observed in release profiles of all NPs can be explained by identical properties and intracellular penetration mechanism. From the data obtained, it can be concluded that PLGA DNR-loaded nanoparticles can be used for overcoming MDR as well as for reducing the frequency of DNR reception due to the prolonged effect, which allows maintaining the concentration of the drug at the required level. The rate of drug administration and the frequency of administration can be calculated based on the DNR release profiles and release parameters.

References

[1] BOHREY S., CHOURASIYA V., PANDEY A., *Polymeric nanoparticles containing diazepam: preparation, optimization, characterization, in-vitro drug release and release kinetic study*, Nano Convergence, 2016, 3(1), 3.

[2] CAPRIOLA A., *Determining an Equilibrium Constant Using Spectrophotometry*, Saint Joseph's University, 2012.

[3] COHENA Y., ISH-SHALOM S., SEGAL E., NUDELMAN O., SHPIGELMAN A., LIVNEY Y., *The bioavailability of vitamin D3, a model hydrophobic nutraceutical, in casein micelles, as model protein nanoparticles: human clinical trial results*, J. Func. Foods, 2017, 30, 321–325.

[4] DUAN J.Z., RIVIERE K., MARROUM P., *In vivo bioequivalence and in vitro similarity factor (f2) for dissolution profile comparisons of extended release formulations: how and when do they match?*, Pharm. Res., 2011, 28(5), 1144–1156.

[5] GAO N., YANG W., NIE H., GONG Y., JING J., GAO L., ZHANG X., *Turn-on theranostic fluorescent nanoprobe by electrostatic self-assembly of carbon dots with doxorubicin for targeted cancer cell imaging, in vivo hyaluronidase analysis, and targeted drug delivery*, Biosens. Bioelectron., 2017, 96, 300–307.

[6] GUIMARAES P.P.G., OLIVEIRAA M.F., GOMES A.D.M., GONTIJO S.M.L., CORTES M.E., CAMPOS P.P., VIANA C.T.R., ANDRADE S.P., SINISTERRAA R.D., *PLGA nanofibers improves the antitumoral effect of daunorubicin*, Colloids Surf B Biointerfaces, 2015, 136, 248–255.

[7] GUKASOVA N.V., ZHUNINA O.A., NIKOLSKAYA E.D., POMAZKOV A.V., SAPELKIN M.A., SEVERIN E.S., TERESHCHENKO O.G., YABBAROV N.G., FIPS 2016118302/15(028761) of 21.03.2017.

[8] GUO M., CHU Z., YAO J., WANG Y., WANG L., FAN Y., *The effects of tensile stress on degradation of biodegradable PLGA membranes: A quantitative study*, Polym. Degrad. Stabil., 2016, 124, 95–100.

[9] HAJAVI J., SANKIAN M., VARASTECH A.-R., HASHEMI M., *Synthesis Strategies for Optimizing Sizes of PLGA Nanoparticles Containing Recombinant Chenopodium Album (rChe a 3) Allergen*, Int. J. Polym. Mater Po., 2017, 66(12), 603–608.

[10] KAITY S., GHOSH A., *Facile preparation of acrylamide grafted locust bean gum-poly(vinyl alcohol) interpenetrating polymer network microspheres for controlled oral drug delivery*, J. Drug. Deliv. Sci. Tec., 2016, 33, 1–12.

[11] KAMALY N., YAMEEN B., WU J., FAROKHZAD O.C., *Degradable controlled-release polymers and polymeric nanoparticles: mechanisms of controlling drug release*, Chem. Rev., 2016, 116(4), 2602–2663.

[12] KAMBUROW M., SIMEONOVA M., *Daunorubicin-loaded chitosan microparticles – preparation and physicochemical characterization*, J. Chem. Technol. Metal., 2016, 51(1), 39–46.

[13] KORSMEYER R., GURNY R., DOELKER E., BURI P., PEPPAS N., *Mechanisms of solute release from porous hydrophilic polymers*, Int. J. Pharmaceut., 1983, 15(1), 25–35.

[14] LAVRIK O.I., *Physical Chemistry of Polymers*, Novosibirsk, 2014.

[15] LIU J., QIU Z., WANG S., ZHOU L., ZHANG S.A., *Modified double-emulsion method for the preparation of daunorubicin-loaded polymeric nanoparticle with enhanced in vitro anti-tumor activity*, Biomed. Mat., 2010, 5, 1–10.

[16] MOHADDESEH M., SABER S., BAHRAINIAN R., DINARVAND F., *Targeted drug delivery of Sunitinib Malate to tumor blood vessels by cRGD-chiotosan-gold nanoparticles*, Int. J. Pharmaceut., 2017, 517(1–2), 269–278.

[17] MOSSMAN T., *Rapid colorimetric assay for cellular growth and survival: application to proliferation and cytotoxicity assays*, J. Immunol. Meth., 1983, 65(1–2), 55–63.

[18] NAGDA C., CHOTAI N.P., PATEL U., PATEL S., SONI T., PATEL P., HINGORANI L., *Mathematical evaluation of similarity factor using various weighing approaches on aceclofenac marketed formulations by model-independent method*, Die Pharmazie, 2008, 63(1), 31–34.

[19] PARHIZKAR M., REARDON P.J.T., KNOWLES J.C., BROWNING R.J., STRIDE E., BARBARA P.R., HARKER A.H., *Electrohydrodynamic encapsulation of cisplatin in poly(lactic-co-glycolic acid) nanoparticles for controlled drug delivery*, Nanomedicine: NBM, 2016, 12(7), 1919–1929.

[20] PAWAR H., WANKHADE S.R., YADAV D.K., SURES S., *Development and evaluation of co-formulated docetaxel and curcumin biodegradable nanoparticles for parenteral administration*, Pharm. Dev. Technol., 2016, 21(6), 725–736.

[21] PEPPAS N.A., *Analysis of Fickian and non-Fickian drug release from polymers*, Pharm. Acta Helv., 1985, 60(4), 110–111.

[22] PIMPLE S., MANJAPPA A.S., UKAWALA M., *PLGA nanoparticles loaded with etoposide and quercetin dihydrate individually: in vitro cell line study to ensure advantage of combination therapy*, Cancer Nanotechnol., 2012, 3(1), 25.

[23] POSADOWSKA U., BRZYCHCZY-WLOCH M., PAMULA E. *Gentamicin loaded PLGA nanoparticles as local drug delivery system for the osteomyelitis treatment*, Acta Bioeng. Biomech., 2015, 17(3), 41–48.

[24] RAHIMI M., MOBEDI H., BEHNAMGHADER A., *In situ-forming, PLGA implants loaded with leuprolide acetate/β-cyclodextrin complexes: mathematical modelling and degradation*, J. Microencapsul., 2016, 33(4), 355–364.

[25] SAHOOO S., CHAKRABORTI C.K., BEHERA P.K., *Development and evaluation of gastroretentive controlled release polymeric suspensions containing ciprofloxacin and carbopol polymers*, J. Chem. Pharm. Res., 2012, 4(4), 2268–2284.

[26] SHARMA D., MAHESHWARI D., PHILIP G., RANA R., BHATIA S., SINGH M., GABRANI R., SHARMA S.K., ALI J., *Formulation and optimization of polymeric nanoparticles for intranasal delivery of lorazepam using Box-Behnken design: in vitro and in vivo evaluation*, BioMed Res. Int., 2014, 3, 1–15.

[27] SUN S.B., LIU P., SHAO F.M., MIAO Q.L., *Formulation and evaluation of PLGA nanoparticles loaded capecitabine for prostate cancer*, Int. J. Clin. Exp. Med., 2015, 8(10), 1967–1981.

[28] TATA D.B., HAHN G., DUNN F., *Ultrasonic absorption frequency dependence of two widely used anti-cancer drugs: doxorubicin and daunorubicin*, Ultrasonics, 1993, 31(6), 447–450.